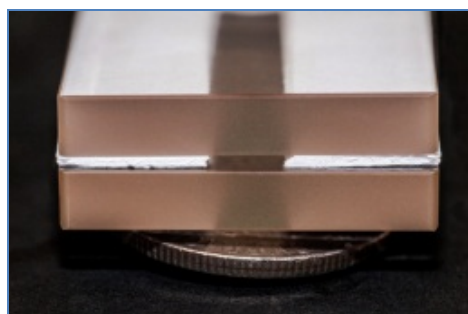




Resurseffektiva kyl- och värmepumpssystem

Studie av värmeförföring, tryckfall och flödesvisualisering vid förångning i små rektagulära kanaler.

Study on heat transfer, pressure drop and flow behavior visualization during evaporation in small channels of a rectangular shape



Förord

The aim of the present study is to prove that the use of small channel heat exchangers in heat pumps and refrigeration equipment can not only minimize the amount of the refrigerant in the system while maintaining the same efficiency of the heat transfer process but also to improve it by achieving higher heat transfer coefficients. This gain is believed to be possible without increase in pressure drop due to the reduction in channel size by use of several parallel channels. It is known from previous studies that the heat transfer coefficients are increasing with reducing the channel diameters. The experimental data are wide and very dependent on the applied conditions but general trend is that decrease in diameter (at least in the range of the application of our interest) is positively influencing the heat transfer coefficient thus making it possible to manufacture more compact heat exchangers for replacing the conventional ones. The results of this study should be used as a base for further manufacturing and test of a heat exchanger that after testing will give a possibility to put the results of the present research into the real values and numbers.

During the implementation of the project the team met significant technical difficulties, such as finding the companies , which can produce the component parts for the test section, long order-delivery time and, most important – it has not yet been found a solution on reading the temperature profiles of the bubble nucleation and growth with the use of Infrared Camera.

Despite these difficulties, the project work was progressing and a significant database of the results was created, resulting into three Master of Science theses, one conference paper, one popular science paper and a submitted journal paper. Three poster presentations and one pitch were held, one of the posters being mentioned among ten best posters and the pitch – among three best pitches at the Energy Day, organized by KTH in the autumn 2013.

Sammanfattning

Kravet på minskning av mängden köldmedium i värmepumpar och kylanläggningar är numera en växande trend. Detta krav är motiverat av flera fördelar bland vilka kan nämnas: minskade utsläpp av köldmedium och därmed minskad påverkan av köldmediet på miljön och omgivningen, minskade kostnader för råmaterialet för tillverkning av en mindre värmeväxlare med samma eller ännu högre effektivitet, minskad utrymme som krävs för systemet, minskade underhållskostnader etc. För att utforma ett system för lägre köldmediemängder bör värmeväxlare med små rördiametrar övervägas. Sådana värmeväxlare har studerats i ett antal forskningsprojekt men kommersiellt finns bara vissa typer av växlare tillgängliga. Ett av de särskilda målen för det föreslagna projektet är att undersöka de tvåfasflödesegenskaperna av köldmedium vid förångning i rektangulära kanaler med olika sidoförhållanden. Den hydrauliska diametern av kanalen är 1253 µm. Det experimentella arbetet har genomförts med en singel- kanal värmeväxlare tillverkad av IR-genomskinligt glas och målet har varit att med IR-kamera studera värmeöverföring i dessa kanaler. Genom jämförelser med resultat från tidigare studier kommer denna studie att bidra till att fastställa vilka korrelationer som kan användas för denna typ av kanaler. Visualisering med en hög hastighet IR-kamera planerades att ge temperaturfördelningen kring bubblorna i flödet och därmed påverkan av den rektangulära kanalformen på värmeöverföringen. Men på grund av vissa tekniska problem beslutades att samla temperaturdata med hjälp av t-typ termoelement placerade på kort avstånd från varandra längs kanalen. Efter projektets slut kan de insamlade uppgifterna användas för det fortsatta arbetet med att utveckla värmeväxlare tillverkade av rektangulära små kanaler och för användning i framtida värmepump- och kylsystem.

Summary

The demand for reduction of the amount of refrigerant charge in the heat pump and refrigeration application is nowadays a growing trend. This demand is motivated by several benefits among which are: the reduced impact of the refrigerant on the environment and surroundings; reduced cost of the primary material for manufacturing of a smaller heat exchanger with the same or even higher efficiency; reduced space necessary for the system installation; reduced run and maintenance costs etc. In order to design a system for lower charges smaller internal volume heat exchangers with reduced tube diameters should be considered. Such heat exchangers have been studied in a few research projects but are not yet generally in commercial use. One of the specific objectives of the proposed project is to investigate the two-phase flow characteristics of the refrigerant evaporating in small rectangular channels with different aspect ratios. The hydraulic diameter of the tested channel is 1253 µm. The experiments were carried out for single-channel heat exchangers made of IR-transparent glass with the scope to collect precise data for heat transfer in these channels. The comparison to previous studies in the field is determining the best predicting correlation for this type of channels and place the collected data in the world-wide database to facilitate studying this still not fully covered topic. Visualization with the high-speed IR camera was planned to provide temperature distribution data around the moving bubbles, important for understanding the evaporation process. However, due to some technical issues it was decided to collect temperature data using t-type thermocouples placed at short distance from each other along the channel. The collected data can be used for further work on developing heat exchangers manufactured from rectangular small channels for implementation in heat pump and refrigeration systems.

Innehåll

Introduction.....	7
1. Literature review.....	10
1.1 Macro to micro-scale transition.....	10
1.2 Flow patterns in micro-channels.....	12
1.3 Flow boiling heat transfer in micro-channels.....	13
1.4 Review of existing correlations for micro-channels.....	14
2. Test rig and test section description.....	17
2.1 Test rig description.....	17
2.2 Test section description.....	18
3. Data reduction	19
3.1 Single-phase data reduction	19
3.2 Two-phase data reduction.....	20
4. Uncertainty analysis.....	22
5. Results and comparisons.....	23
5.1 Single-phase tests and results.....	23
5.2 Two-phase tests and results	28
6. Conclusions.....	33
Referenses.....	36
Projektets vetenskapliga publikationer.....	40
Projektets populärvetenskapliga publikationer och presentationer.....	41
APPENDIX 1 Nomenclature.....	42

Introduction

The environmental concern is one of the several reasons for the increasing application of compact heat exchangers. According to the Montreal Protocol, CFC refrigerants have been banned from the market in most developed countries of the world, due to the harmful effect of chlorine on the ozone layer. For the same reason, their temporary substitutes HCFCs are being phased out in many countries, at different timetables. Nowadays synthetic HFCs are widely used; they do not contain chlorine but do have a high global warming potential (GWP). Therefore, it might be likely to have new legislations in the next period in order to stop their future development. Of course there are some alternatives to synthetic refrigerants, such as ammonia and non-halogenated hydrocarbons (HC), already used for several applications. Although these natural refrigerants are not dangerous for the environment (or at least the influence of these fluids is negligible), they still present some problems, such as toxicity for ammonia and flammability for hydrocarbons.

Thus, independently of which type of refrigerant is used, it is important to lower emissions due to inevitable leakages from refrigerating systems. Working with small internal volume heat exchangers allows reducing the charge of refrigerant in the system, thus limiting the above mentioned damages and bringing beneficial on fluid charging costs.

Apart from the direct greenhouse effect caused by leakages from refrigerating systems, another type of concern is due to the so called "indirect greenhouse gas emissions" connected to the use of electricity (the production of which is frequently connected to fuel combustion). Generally, performance improvements are achieved by increasing the heat transfer coefficient between the fluid and the wall surface, which in turn augments the thermodynamic efficiency and reduces the operating costs.

In this context, numerous studies point out that boiling mechanism in mini and micro-channels appears to be different from conventional macro-channels, leading to an enhancement of the heat transfer coefficient. As a matter of fact, the heat transfer process in micro-channels depends on the heat transfer surface area, which varies linearly with the channel hydraulic diameter (D_h). The mass flow rate, on the other hand, depends on the cross-sectional area of the channel, which varies linearly with D_h^2 . Hence the heat transfer surface area to volume ratio varies as $1/D_h$. As the hydraulic diameter decreases, the ratio increases. In laminar flow for a micro-channel, the local heat transfer coefficient varies inversely with the channel diameter. Therefore, as the channel diameter decreases, the heat transfer coefficient increases, improving both the compactness of the unit as well as the heat transfer rate.

Furthermore, miniaturization of heat exchangers is a trend that fits well into the field of electronic cooling. The size of electronic devices has decreased surprisingly in the last decades, and this has made possible to obtain faster chip speeds but at the same time has led to greater chip power densities. Consequently, recent developments in the field

of microelectronics due to miniaturization have resulted in dissipation of much higher heat fluxes than ever before, exceeding the fan cooling limits. Heat fluxes generated in microelectronics have reached about 100 W/cm^2 today and this number keeps rising up to $200\text{-}300 \text{ W/cm}^2$ to be achieved in near future. The surface temperature of high heat dissipating microchips ought to be maintained below 85°C in order to ensure the effectiveness of the electronic circuitry. Therefore, new technologies for thermal management need to be developed in order to promote the miniaturization process. For this reason, micro-channel heat sinks have received much attention for their very promising cooling potential, as they allow attainment of significantly higher heat flux level in two-phase flows, if compared with conventional circular tube exchangers. This is due to a higher heat transfer surface area density achievable with compact evaporators.

The application of micro-channels is not only limited to microelectronics industry, in fact there are several other application areas which can benefit from the advantages given by micro-channel technology. Miniaturized heat exchangers may be used in automotive industry to reduce the refrigerant charge, comparing them to conventional sized heat exchangers for the same heat transfer performance. Heat pump industry is a potential application area for compact heat exchangers which employ micro-channels. Again, the compact and efficient evaporators and condensers will increase the performance of the refrigeration system, reducing at the same time the fluid charge.

Advantages of micro-channels common to all the above mentioned applications are listed below:

- Larger heat transfer surface area and higher surface-area-to-volume ratio, thus a higher cooling potential;
- Enhanced heat transfer coefficient, if compared to conventional sized heat exchangers;
- Compactness and light weight;
- Reduction of the fluid charge, resulting in minor operating costs and helpful towards environmental issues;
- Compact size is (although not always) associated with relatively low capital cost. At least installation costs are reduced if the size of a component is reduced.

Despite all these advantages of using micro-channels, some issues still remain. First of all the pressure drop in mini or micro-channels is higher than that which occurs with a conventional tube, because of the increased wall friction. Excessive pressure drop is always a concern, since these devices are typically used with miniature pumps with limited pumping power capability. Another practical concern is pressure oscillation due to hydrodynamic instabilities, which must be therefore identified and prevented to ensure safe operation and predictable cooling performance.

Furthermore, the research about micro-channels for thermal and other engineering applications is relatively recent. Still, applications of micro-channels can not only be found in laboratories, but also in the form of heat pipes in consumer electronics, in the

automotive industry where miniaturized heat exchangers are used as condensers for AC systems and to a much lesser extent in the refrigeration industry. Still, the mass production and application of micro-channels is not very common in the commercial market yet, and this is possibly due to: the lack of availability of adequate data and design correlations in the open literature; insufficient understanding of heat transfer and fluid flow behaviours in micro-channels. In fact, what can now be fabricated in micro-scale has vastly outpaced what can be thermally modelled.

In the last years, a large number of experiments on two-phase flow and heat transfer in mini and micro-channels have been performed. Despite the large discrepancy existing among different results published, it appears that boiling heat transfer, pressure drop and flow patterns in micro-channels cannot be properly explained with the existing macro-scale correlations. The well-established explanation for this difference is that the physical mechanisms that are potentially dominant in micro-channels are less important in macro-channels. The unsolved issues are partially due to the difficulty to define precisely the threshold between micro and macro-scale and therefore the lower limit from which the macro-scale correlations are applicable. As a summary, physical phenomena are not well understood yet and before making any confident prediction of heat transfer rate in micro-channels, more experimental data is needed to solve the discrepancy in literature.

1. Literature review

Leaving aside all the theory regarding pool boiling and flow boiling in conventional channels, this literature review will focus on flow boiling in small channels only.

1.2 Macro to micro-scale transition

The transition between the macro and micro scale in boiling has been observed by several authors and according to different parameters such as flow pattern, heat transfer coefficient, critical heat flux (CHF), void fraction etc. It has been proven that calculation and prediction methods for boiling flows in conventional channels cannot be applied to mini channels environment.

Four forces are influencing two-phase flow in channels: gravitational, inertia, viscous and surface-tension. The main reason of the difference between macro and micro-scale behavior is the relative significance of these forces, which are included in different dimensionless numbers: Bond and Reynolds numbers. Bond number (Bo) is a measure of the importance of gravitational forces compared to surface tension forces. A high Bond number indicates that the system is almost unaffected by surface-tension effects, whereas a low Bond number indicates that surface tension dominates over gravitational effects. As the channel hydraulic diameter decreases, the bubbles are squeezed in the flow channel and the surface tension gradually dominates the flow. Thus, the heat transfer mechanisms deviate from those of conventional channels and micro-scale behavior will occur. On the other hand, the Reynolds number (Re) measures the ratio of inertia forces to viscous forces and thus quantifies the relative importance of these two forces for a given flow condition. It is well-known that laminar flow occurs at low Reynolds numbers where viscous forces are dominant, while turbulent flow occurs at high Reynolds numbers, where the flow regime is dominated by inertia forces. In micro-channels, the narrow diameter makes liquid Reynolds numbers smaller than the critical one; hence in evaporative boiling saturated liquid flows as a laminar flow, whereas in conventional channels saturated liquid flows in the turbulent region.

Several classifications for the transition from macro to micro-scale have been proposed. Some of them are based on dimensionless numbers, while other methods are based only on the hydraulic diameter of the channel.

Mehendale et al. (2000) recommended a size classification based on the hydraulic diameter as follows: conventional channels ($D_h > 6 \text{ mm}$); compact heat exchangers ($1 - 6 \text{ mm}$); meso-channels ($100 \mu\text{m} - 1 \text{ mm}$); micro-channels ($1 - 100 \mu\text{m}$).

Kandlikar and Grande (2003) suggested instead this classification: micro-channels (50 – 600 µm); mini-channels (600 µm – 3 mm) and conventional channels ($D_h > 3$ mm). These two criteria are arbitrary and do not reflect the influence of channel size on the physical mechanisms.

Kew and Cornwell (1997) recommended using a confinement number (Co), which almost reproduces the Bond number defined above, as a criterion for defining the channels as macro or micro-scale. They observed that the surface tension becomes important and the effects of gravity diminish when reducing the channel size. The confinement number is defined as:

$$Co = \left(\frac{1}{Bo} \right)^{\frac{1}{2}} = \left[\frac{\sigma}{g \cdot (\rho_L - \rho_G) \cdot D_h^2} \right]^{\frac{1}{2}} \quad (3.43)$$

They reported that the heat transfer and the flow characteristics in channels with $Co > 0,5$ were significantly different than those observed in macro-channels, where $Co < 0,5$. Hence the threshold between macro and micro-scale is represented by the value 0,5 for the confinement number.

Thome et al. (2004) suggested the confined bubble as the threshold to define the transition from macro to micro-scale: this criterion is related to the bubble departure diameter. In narrow tubes the bubble departure diameter reaches that of the channel, thus further growth is confined by the channel and only one bubble can exist in the channel cross section at a time (whereas multiple bubbles are present in a conventional channel). Fritz' equation (1935) gives the bubble departure diameter:

$$d_0 = 0,0208 \cdot \beta \cdot \left[\frac{\sigma}{g \cdot (\rho_L - \rho_G)} \right]^{\frac{1}{2}} \quad (3.44)$$

where β is the contact angle in degrees (°).

Brauner and Maron (1992) proposed a criterion in terms of Bond number for the importance of surface tension upon the gravity effects. They suggested a critical value of $Bo = 2\pi$ below which the channel may be classified as micro-channel.

Harirchian and Garimella (2010) suggested another criterion based on a convective confinement number, which is defined as $Bo^{0,5} \cdot Re$, where Bo is the boiling number. The authors proposed a critical value of 160 for convective confinement number below which the channel should be classified as micro-channel.

From what has been written, it is interesting to note that there still doesn't exist a well-established criteria to define a threshold for transition from macro to micro-scale channels.

1.2 Flow patterns in micro-channels

Flow patterns for micro-channels might be quite different from those in conventional channels. First of all, one important difference with respect to macro-channels flow is that the liquid flow is almost always laminar, due to the narrow diameter of the tube, and this behavior is quite rare in macro-channels studies. Hence, flow pattern transition theories for turbulent liquid flows may not be applied for laminar conditions.

Another important point is that capillary forces (surface tension effects) become more important in small diameter tubes, leading to a minor or negligible stratification of the liquid. Channel orientation is thus no longer of primary importance when dealing with micro-channels.

Before illustrating some two-phase flow studies in narrow tubes, it is important to state that, as happened in conventional channels, flow pattern observations are subjective and various researchers use different categories or names to describe the same thing, or use additional subcategories that other do not.

Palm (2002) observed only three flow patterns: isolated bubble flow, where bubbles are still smaller than the channel diameter; confined bubble flow, where the bubble diameter is restricted by the diameter of the tube; and annular flow.

Feng and Serizawa (2000) used an adiabatic mixture of air-water in a 50 µm diameter and categorized their observations as follows: bubble flow, elongated bubble flow (with the same meaning as the confined bubble flow), annular flow and liquid ring flow, which can be defined as an additional flow pattern between elongated bubble flow and annular flow and thus it seems to be some type of intermediate transition regime.

Tran et al. (1996) studied two-phase flow patterns for R-12 in a 2,46 mm circular channel, noting that the transition from elongated bubble flow to annular flow occurred at much higher vapor qualities ($x \approx 0,6-0,7$) than those typical of macro-channels ($x \approx 0,25-0,35$).

Kuwahara et al. (2000) investigated R-134a evaporating in a 1,2 mm horizontal tube. They observed flow regimes typical of macro-scale theory: bubbly flow, plug flow, slug flow, wavy-annular flow and annular flow.

Kew and Cornwell (1997) identified three different flow regimes in their work: isolated bubbles, confined bubbles and an annular flow regime plus partial dryout at some conditions. The boiling was found to be very unstable as the formation of bubbles pushed the liquid slugs forward in the channel. Thus there is a risk that the average heat transfer coefficient may be affected by instability due to intermittently dry surfaces in part of the tube.

Recently, Callizo et al. (2010) performed studies in a vertical circular channel having a diameter of 1,33 mm and R134a as working fluid. They recognized seven distinct flow patterns: bubbly, elongated bubbly, slug, churn, slug-annular, annular and mist flow.

They also noticed that higher saturation pressures shifted the transition boundaries to higher vapor qualities.

It can finally be observed that for evaporating flows, the bubbly flow regime is very short as bubbles grow fast up to the size of the channel, typically within a few centimeters of tube length or even less. Many other flow pattern observations are reported in literature for micro-scale two-phase flows, but to capture most of the physics involved it seems sufficient to recognize only bubbly, elongated bubble, annular and flow with partial dryout as the leading regimes.

1.3 Flow boiling heat transfer in micro-channels

This section aims to describe some flow boiling heat transfer studies reported in literature.

Tran et al. (1996) performed evaporating tests in a circular channel of 2,46 mm diameter. They noticed that the local heat transfer coefficients did not change with mass flux or with vapor quality, but were dependent on heat flux. As a consequence, they stated that micro-channel evaporation was always dominated by nucleate boiling.

Zhao et al. (2000) studied flow boiling in a micro-channel of unspecified dimensions. No mass flux dependence was observed on the heat transfer coefficients for either CO₂ or R134a. In contrast to the study above, their results did not show any heat flux dependence.

Bao et al. (2000) calculated local flow boiling coefficients for R11 and R123 inside a 1,95 mm copper tube. They observed that heat transfer coefficients were a strong function of heat flux and increased with saturation pressure, whereas the effects of mass flux and vapor quality were negligible. Hence they concluded that nucleate boiling dominated the heat transfer process. They also noted that the Cooper correlation gave an approximate representation of their data.

Hwang et al. (2000) measured flow boiling heat transfer coefficients for R134a in a 2,2 mm steel tube. They classified most of the experimental data in slug and annular flow regimes. For a wide range of vapor quality, their results showed an influence of heat flux but also an effect of mass flux. Hence there was no certainty about the dominance of the nucleate boiling mechanism in their tests.

Lin et al. (2001) studied evaporation of R141b in a vertical 1,1 mm tube. As opposed to most of previous studies, they found a significant influence of vapor quality on the heat transfer coefficients. For low heat fluxes, there was a monotonic rise in values up to a peak at about $x = 0,60$; for intermediate heat fluxes the heat transfer coefficients were almost independent on vapor quality. At high heat fluxes, instead, their results showed a peak at low vapor qualities and then a monotonic decrease.

Maqbool et al. (2013) investigated flow boiling heat transfer of propane in a vertical stainless steel channel having an internal diameter of 1,70 mm and a heated length of 245 mm. They observed the heat transfer coefficients increasing with the increase of heat flux and saturation pressure, while the influence of mass flux and vapor quality was insignificant. This behavior made them conclude that a nucleate boiling mechanism played a major role and convective boiling was of minor importance in micro-channels.

Summarizing the results above, most of them claim that flow boiling heat transfer coefficients in micro-channels are not a function of mass flux or vapor quality (and this is in contrast with macro-scale theory), but they are a function of heat flux and saturation pressure. Hence flow boiling in micro-channels is controlled by nucleate boiling. On the other hand, Hwang et al. (2000) and Lin et al. (2001) studies showed a significant effect of mass flux, respectively, whereas Zhao et al. (2000) observed a heat flux negligible influence on the heat transfer coefficient. For this reason, a complete picture of the flow boiling mechanism in micro-channels has not been established yet.

Furthermore, a research performed by Jacobi and Thome (2002) claims that nucleate boiling is not the dominant heat transfer mechanism in micro-channels. They concentrated on the transient thin film evaporation phenomenon in the liquid film trapped between the wall and the passing bubbles. Although their two-zone model was only partially completed (and then they developed a new three-zone model), this approach was useful for them to state that micro-channel heat transfer is largely influenced by the transient film evaporation mechanism and not simple nucleate boiling.

1.4 Review of existing correlations for micro-channels

This sub-section presents some of the correlations developed specifically for micro-channels. Most of them have been used as a comparison with this reports' data.

Lazarek and Black (1982) investigated saturated flow boiling of R113 in a 3,15 mm inner diameter tube. They found out that the heat transfer coefficients showed a strong dependence on heat flux with negligible influence of vapor quality, suggesting that the mechanism of nucleate boiling controlled the heat transfer process. The authors proposed a simple correlation:

$$h_{tp} = 30 \cdot Re_L^{0,857} \cdot Bo^{0,714} \cdot \frac{\lambda_L}{D_h}$$

Kandlikar (1990) proposed a new correlation based on 10000 data points covering water, refrigerants and cryogenic fluids. For vertical tubes, the expression is:

$$\text{if } Co < 0,65 \rightarrow h_{tp} = [1,136 \cdot Co^{-0,9} + 667,2 \cdot Bo^{0,7} \cdot F_{fl}] \cdot 0,023 \cdot Re_L^{0,8} \cdot Pr_L^{0,4} \cdot \frac{\lambda_L}{D_h}$$

$$\text{if } Co > 0,65 \rightarrow h_{tp} = [0,6683 \cdot Co^{-0,2} + 1058 \cdot Bo^{0,7} \cdot F_{fl}] \cdot 0,023 \cdot Re_L^{0,8} \cdot Pr_L^{0,4} \cdot \frac{\lambda_L}{D_h}$$

where F_{fl} is the fluid-surface parameter, and its value is 1,63 for R134a.

Tran et al. (1996) performed boiling heat transfer experiments of R12 in narrow tubes. Considering the dominant mechanism to be nucleate boiling rather than convective evaporation, the authors proposed the following correlation:

$$h_{tp} = 8,4 \cdot 10^5 \cdot Bo^{0,6} \cdot We_L^{0,3} \cdot \left(\frac{\rho_L}{\rho_G}\right)^{-0,4}$$

where We is the Weber number: $We = \frac{G^2 \cdot D_h}{\rho \cdot \sigma}$.

Kew and Cornwell (1997) suggested a modified Lazarek and Black equation, to allow for an observed increase in the heat transfer coefficient with the vapor quality, as it happens in larger tubes:

$$h_{tp} = 30 \cdot Re_L^{0,857} \cdot Bo^{0,714} \cdot (1 - x)^{-0,143} \cdot \frac{\lambda_L}{D_h}$$

Yu et al. (2002) followed the same approach of Tran et al. and proposed a modified correlation as follows:

$$h_{tp} = 6,4 \cdot 10^6 \cdot (Bo^2 \cdot We_L)^{0,27} \cdot \left(\frac{\rho_L}{\rho_G}\right)^{0,2}$$

Warrier et al. (2002) conducted saturated nucleate boiling experiments in small rectangular channels, using FC-84 as working fluid. They proposed a correlation which is only dependent on the vapor quality and the boiling number:

$$h_{tp} = \left[1 + 6 \cdot Bo^{\frac{1}{16}} - 5,3 \cdot (1 - 855Bo) \cdot x^{0,65} \right] \cdot 0,023 \cdot Re_L^{0,8} \cdot Pr_L^{0,4} \cdot \frac{\lambda_L}{D_h}$$

Owhaib (2007) developed a correlation based on data obtained for R134a in vertical circular micro-channels, for several flows and tube diameters:

$$h_{tp} = 400 \cdot (Re_L \cdot Bo)^{0,5} \cdot (1 - x_{ex})^{0,1} \cdot Co^{0,55} \cdot P_r^{1,341} \cdot \left(\frac{\rho_L}{\rho_G}\right)^{0,37} \cdot \frac{\lambda_L}{D_h}$$

Based on the Lazarek and Black correlation and by introducing the Weber number, Sun and Mishima (2009) proposed a modified correlation, using a new database including 2505 data points for 11 fluids and covering diameters from 0,21 up to 6,05 mm:

$$h_{tp} = \frac{6 \cdot Re_L^{1,05} \cdot Bo^{0,54}}{We_L^{0,191} \cdot \left(\frac{\rho_L}{\rho_G} \right)^{0,142}} \cdot \frac{\lambda_L}{D_h}$$

More recently, Li and Wu (2010) collected saturated flow boiling experiments from the literature, filling a database with more than 3700 data points, covering a wide range of working fluids, operational conditions and different channel dimensions. Using the boiling number, the confinement number and Reynolds number, the authors developed a new general correlation for evaporative heat transfer in mini/micro-channels:

$$h_{tp} = 334 \cdot Bo^{0,3} \cdot \left(\frac{1}{Co^2} \cdot Re_L^{0,36} \right)^{0,4} \cdot \frac{\lambda_L}{D_h}$$

2. Test rig and test section description

2.1 Test rig description.

The Fig.1 represents a sketch of the test rig where main components of the test facility are an evaporator (test section), a condenser and a pump. The system is equipped with the necessary measurement devices: an absolute pressure transducer to measure the system pressure at the inlet of the test section; one differential pressure sensor to measure the pressure drop across the test section; multiple thermocouples (T-type) to determine fluid and wall temperatures; one mass flow meter to measure the flow rate; current and volt meters, essential to get the heat power injected into the test section.

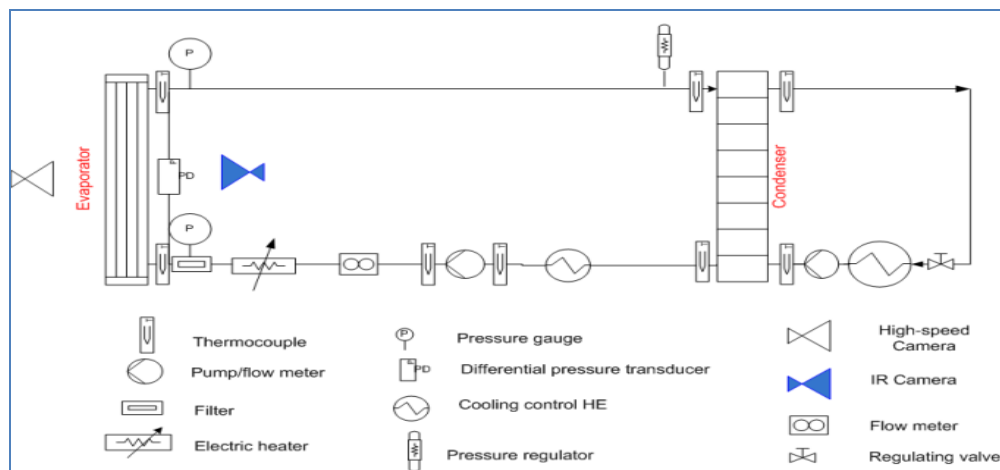


Fig.1. Schematic representation of the experimental facility

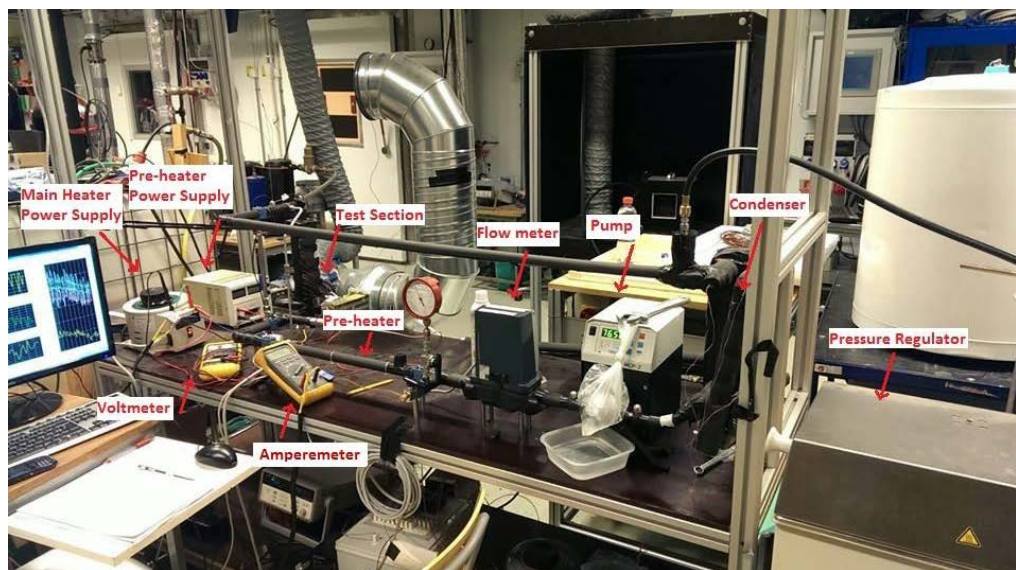


Fig.2. Photo of the experimental facility

All measuring equipment was carefully calibrated. R134a is the working fluid, whereas a mixture of water/glycol is used in the secondary loop to cool down the condenser. The electrical pre-heater is used for setting the necessary entrance conditions of the working fluid. The system pressure is regulated by setting the temperature of a tank, placed in a thermostatically-controlled water bath, connected to the main loop.

2.2 Test section description

Both sides of the test section are made of sapphire glass plates. These plates with the dimensions 190x30x5 mm are coated with a 6 mm wide strip of indium-tin oxide (ITO) down in the middle of each plate on the channel side. Current applied to the coating allows the fluid in the channel to be heated. The channel is formed in between those two plates, where its height is determined by the thickness of the Teflon layer. The plates' frame is made up of Aluminum and allows the visualization of the channel from both sides.

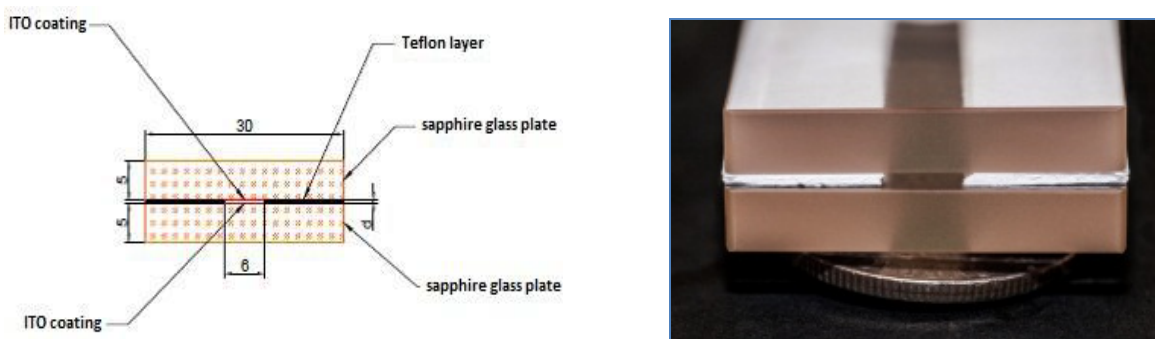


Fig.3. Photo and the cross-cut of the test section

The channel has a rectangular shape, and its dimensions are:

Width: 6mm

Length: 190mm

Height: 0,7mm

These dimensions correspond to the hydraulic diameter of

$$D_h = 4 \cdot \frac{A}{\Psi} = 1,253 \text{ mm}$$

Where Ψ is the cross section perimeter and A the cross section itself.

The channel has an aspect ratio of $a_r = \frac{\text{width}}{\text{height}} = 8,571$.

3. Data reduction

3.1 Single-phase data reduction

The heat flux transmitted can be evaluated as follows:

$$q'' = \dot{m} \cdot c_p \cdot \frac{T_{fluid,out} - T_{fluid,in}}{\text{Heated Surface}} \quad \left[\frac{W}{m^2} \right]$$

The mass flow rate \dot{m} is one of the measured parameters;

$T_{fluid,in}$ and $T_{fluid,out}$ are the measured fluid temperatures at the inlet and the outlet of the evaporator section, respectively.

The heat capacity c_p , as the other thermodynamic properties that follow, is calculated at the measured test section inlet pressure and at the average temperature

$$T_{fluid,mean} = \left(\frac{T_{fluid,in} + T_{fluid,out}}{2} \right).$$

The Heated Surface is the sapphire's area covered with the ITO coating.

The mean heat transfer coefficient can be estimated with the Newton's law:

$$h_{mean} = \frac{q''}{T_{inwall,mean} - T_{fluid,mean}} \quad \left[\frac{W}{m^2 K} \right]$$

$T_{inwall,mean}$ is the inner mean wall temperature. It can be calculated using Poisson equation from the measured outside wall temperature considering these simplified hypothesis:

1. Linear heat transfer through the wall, as the glass thickness is much smaller than its width and length.
2. Uniform heat generation u''' .
3. Steady conditions.
4. Outer wall perfectly insulated.

$$T_{inwall,mean} = T_{outwall,mean} - \frac{u'''}{2\lambda_{sap}} \cdot s^2$$

The mean outer wall temperature $T_{outwall,mean}$ can be calculated with the arithmetic average of the measured values supplied with the 9 thermocouples on the test section.

In the single phase flow experiments, the temperature of the liquid is always kept below the saturation temperature corresponding to the actual pressure.

Once h_{mean} has been established, it is traditionally expressed in its dimensionless form by means of the Nusselt number, Nu_{mean} , which may be defined as the ratio of convection heat transfer to conduction heat transfer under the same conditions with the expression:

$$Nu_{mean} = \frac{h_{mean} D_h}{\lambda} \quad [-]$$

where D_h is the hydraulic diameter and λ is the fluid thermal conductivity.

To get the local heat transfer coefficient along the test section, we assume the fluid temperature increases linearly along the heated test section (uniform heat flux), thus the bulk fluid temperature at any axial position z , $T_{fluid}(z)$, can be calculated as:

$$T_{fluid}(z) = T_{fluid,in} + (T_{fluid,out} - T_{fluid,in}) \cdot \frac{z}{L}$$

where L is the whole channel length (190 mm).

Then we can use the same formula achieved with the average values, this time with local values:

$$T_{inwall}(z) = T_{outwall}(z) - \frac{u'''}{2\lambda_{gap}} \cdot s^2$$

The outer wall temperatures $T_{outwall}(z)$ are taken directly from the thermocouples glued on the test rig.

Hence the local heat transfer coefficient is given by:

$$h(z) = \frac{q'''}{T_{inwall}(z) - T_{fluid}(z)} \quad \left[\frac{W}{m^2 K} \right]$$

As regard the experimental pressure drop, the differential pressure sensor is able to show the requested values outright.

3.2 Two-phase data reduction

$T_{fluid,in}$ and $T_{fluid,out}$ are the measured fluid temperatures at the inlet and the outlet evaporator section, respectively.

For a given test point, the heat flux added to the test section, q'' , is calculated as:

$$q'' = \frac{VI}{A} \quad \left[\frac{W}{m^2} \right]$$

where V and I are the voltage and the current applied to the test section, respectively, and A is the heated surface. It is assumed that the heat flux is evenly distributed across

the surface. Local heat transfer coefficients are calculated from the measured wall and bulk temperatures, as:

$$h(z) = \frac{q^*}{T_{wall,in}(z) - T_{fluid}(z)} \quad \left[\frac{W}{m^2 K} \right]$$

where internal wall temperature ($T_{wall,in}(z)$) is calculated from the measured external wall temperature with the steady state one-dimensional heat conduction equation with heat generation. The assumptions are as follows: linear heat transfer through the wall (as the glass thickness is much smaller than its width and length); uniform heat generation; steady-state conditions; perfectly insulated outer wall. $T_{fluid}(z)$ is the local fluid bulk temperature, calculated from the inlet and outlet temperature values with the assumption of linear variation along the test section (for both subcooled region and boiling region). As the saturation temperature drop is usually less than 0,5 K this assumption introduces an error much smaller than the accuracy in the temperature measurement.

The axial position along the channel where saturation conditions are reached has to be known; therefore the subcooled length (Z_0) is calculated with an energy balance for the liquid region:

$$Z_0 = \frac{\dot{m}c_p(T_{sat,in} - T_{fluid,in})}{q^*\psi} \quad [m]$$

where \dot{m} is the measured mass flow rate, c_p is the specific heat, $T_{sat,in}$ is the saturation temperature at the measured inlet pressure, $T_{fluid,in}$ is the measured temperature at the inlet of the test section and ψ is the perimeter of the cross section.

With the abovementioned assumptions, $T_{fluid}(z)$, the local fluid temperature in the boiling region is calculated as:

$$T_{fluid}(z) = T_{sat,in} - \left(\frac{T_{sat,in} - T_{fluid,out}}{Z_{tot} - Z_0} \right) * (z - Z_0) \quad [{}^\circ C]$$

where $T_{fluid,out}$ is the measured temperature of the fluid at the outlet of the test section and Z_{tot} is the total length of the heated section.

Once the local heat transfer coefficient has been evaluated, the average heat transfer coefficient is determined arithmetically averaging the local values along the channel.

The vapour quality at any point along the channel is determined from the energy balance over the boiling region:

$$x(z) = \frac{q^*\psi(z - Z_0)}{\dot{m}h_{fg}} \quad [-]$$

In the latest equation h_{fg} is the latent heat of vaporization

4. Uncertainty analysis

Uncertainty of a measured or a derived parameter defines a range where the actual or correct value is most probable to lie. The results of the uncertainty analysis performed in the present study are presented in the Table 1.

Uncertainties of measured parameters		Uncertainties of derived parameters	
Parameter	Uncertainty	Parameter	Uncertainty
Temperature, T	± 0,1°C	Saturation temperature, T _{sat}	± 0,8°C
Pressure, P	± 16 mbar	Mass flux, G	± 3%
Differential pressure, ΔP	±0,5 mbar	Heat flux, q"	± 3%
Mass flow rate, \dot{m}	± 2%	Enthalpy, h	± 10%
Voltage, V	± 0,14%	Vapor quality, x	± 3÷5%
Current, I	±0,8%		
Thermal Properties	± 2%		

Table 1. Summary of systematic uncertainties for the measured and derived parameters

5. Results and comparisons

5.1 Single-phase tests and results

Single-phase tests were mainly performed to validate the test section, the whole instrumentation, heat losses and the overall system performance. The secondary objective was to verify that classical correlations utilized for tubes with conventional diameters are effective for narrow pipes as well. For this reason, the single-phase heat transfer and pressure drop results are compared with existing formulas. The operating conditions for single-phase tests are summarized in the Table 2.

Parameter	Operational data range
P_{in} [bar]	6.9-7.07
G [kg/m ² s]	80-333
q'' [kW/m ²]	0.656 – 1.03

Table 2. Operating conditions for single-phase experiments

The system pressure has been fixed to 7 bar and seven different mass flow rates have been chosen, from 0.75 g/s up to 2 g/s, covering the entire range supplied by the electric pump. For four mass fluxes, the heat flux has been gradually increased up to the saturation limit, which has never been achieved. The highest heat flux at the wall has been chosen to ensure a subcooling degree of no less than 3°C at the outlet of the test section; that is to guarantee that the bulk temperature of the working fluid was never allowed to exceed the saturation temperature corresponding to the system pressure.

Single-phase heat transfer

The Reynolds number influence on the average heat transfer coefficient and thus the average Nusselt number is clearly seen from the Fig.4 below; where heat flux q is measured in W/m².

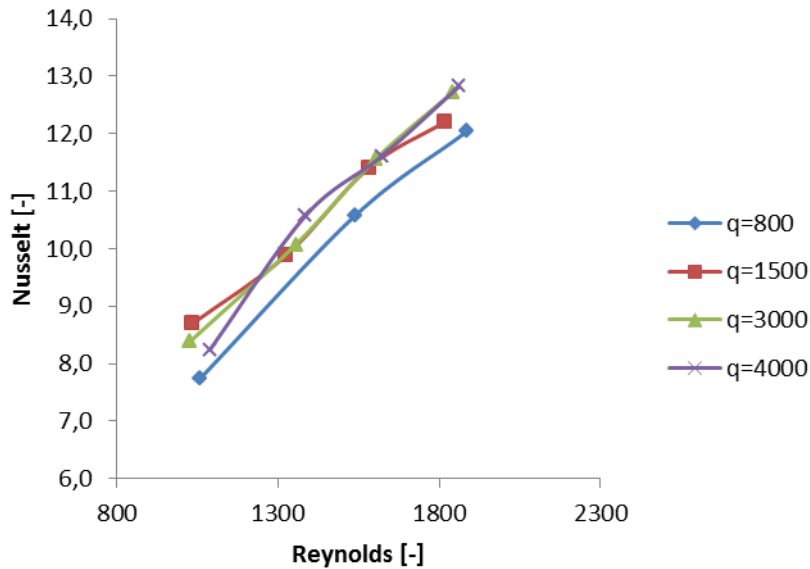


Fig.4. Experimental average Nusselt number as a function of the Reynolds number for several heat fluxes

Mass flux (and thus Reynolds number) has a strong influence on the average Nusselt number. Furthermore, as expected, the curves seem to blur for all the Reynolds numbers, verifying the trends just seen before.

To determine if classical correlations developed for conventional pipes are in agreement with the experimental results, as an example, figures 5 and 6 show the experimental Nusselt numbers as a function of the heat flux at mass fluxes $G = 287 \text{ kg/m}^2\text{s}$ and $G = 333 \text{ kg/m}^2\text{s}$. These values are therefore compared with some of the classical correlations developed for conventional pipes already seen in the previous section.

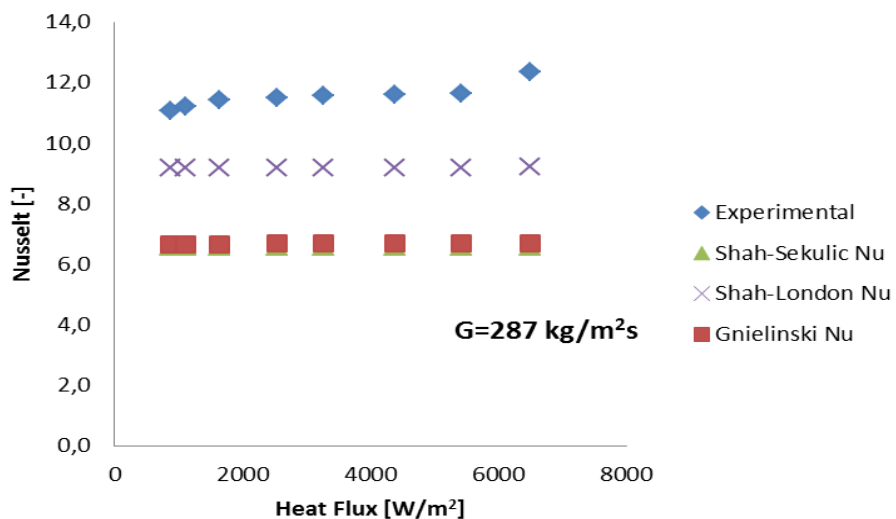


Fig.5. Comparison for the experimental Nusselt with macro-scale correlations at fixed $G = 287 \text{ kg/m}^2\text{s}$

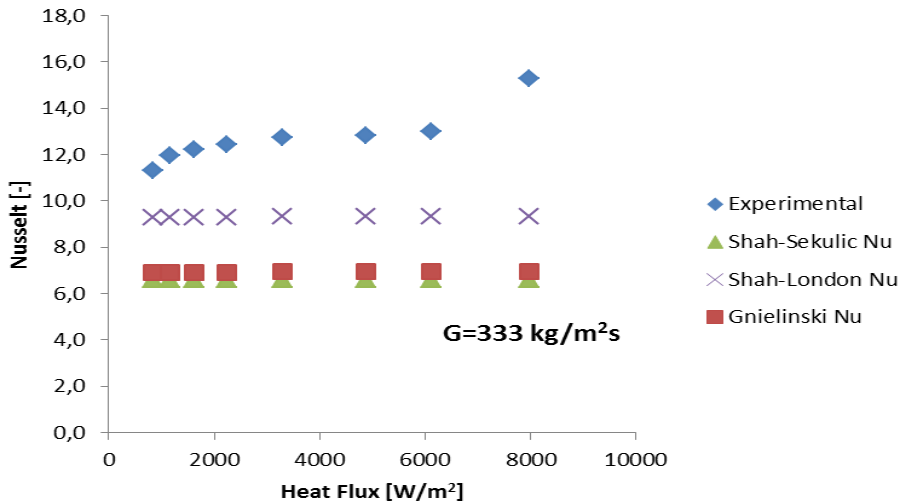


Fig.6 Comparison for the experimental Nusselt with macro-scale correlations at fixed $G = 333 \text{ kg/m}^2\text{s}$

All the correlations underestimate the experimental average Nusselt. However it seems that data tends to get closer to the Shah-London correlation, whereas they are pretty far from Shah-Sekulic and Gnielinski predicted values.

The experimental data shows a faster increase than the theoretical prediction results. Only Gnielinski (1995) seems to consider an important increase of the Nusselt number with the Reynolds.

Finally, the local heat transfer coefficient for different mass and heat fluxes is shown in Fig.7. As it can be seen, the local heat transfer coefficient increases along the channel; that is because the difference between the wall temperature and the bulk fluid temperature gradually decreases from the inlet up to the outlet section.

Considerations made for the average Nusselt are consistent with the local values: the heat transfer coefficient is increasing with mass flux (and thus the Reynolds number), whereas the curves with same mass flux and different heat flux are about to merge together.

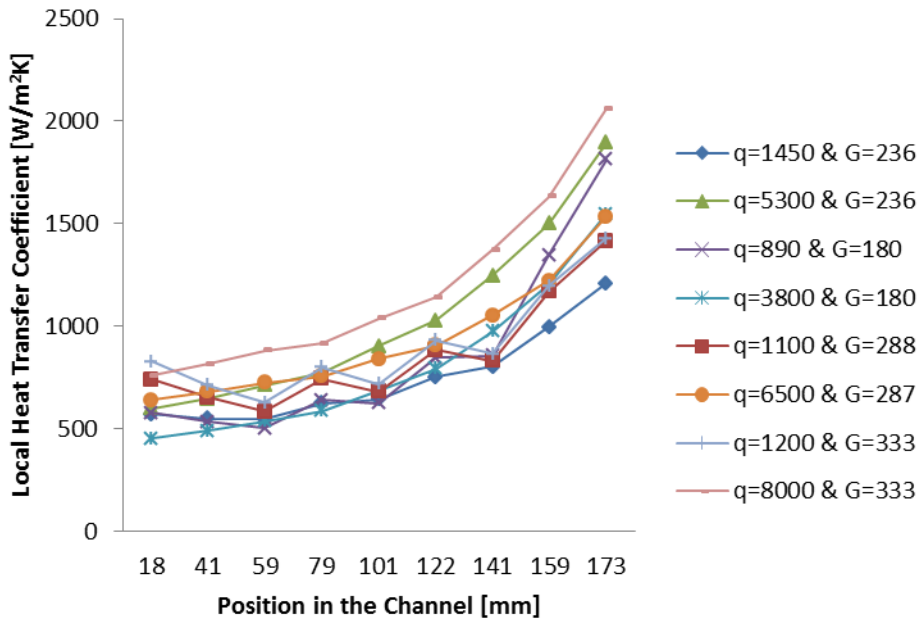


Fig.7. Distribution of the local heat transfer coefficient as a function of the axial position, for several heat and mass fluxes

Single-phase pressure drop

In Fig.8 experimental pressure drops are compared with the values obtained from the classical expression:

$$\Delta P = 2f \cdot \frac{L_{eq}}{D_h} \cdot \frac{G^2}{\rho}$$

with L_{eq} the equivalent test section length (considering the two elbows between the differential pressure transducer). The Fanning factor f is computable as $\frac{Po}{Re}$, where Po is the Poiseuille dimensionless number. According to Thome (2004-2010 a), for a rectangular channel with an aspect ratio close to $\frac{1}{8}$ and in laminar flow conditions, Po should be chosen equal to 20,585.

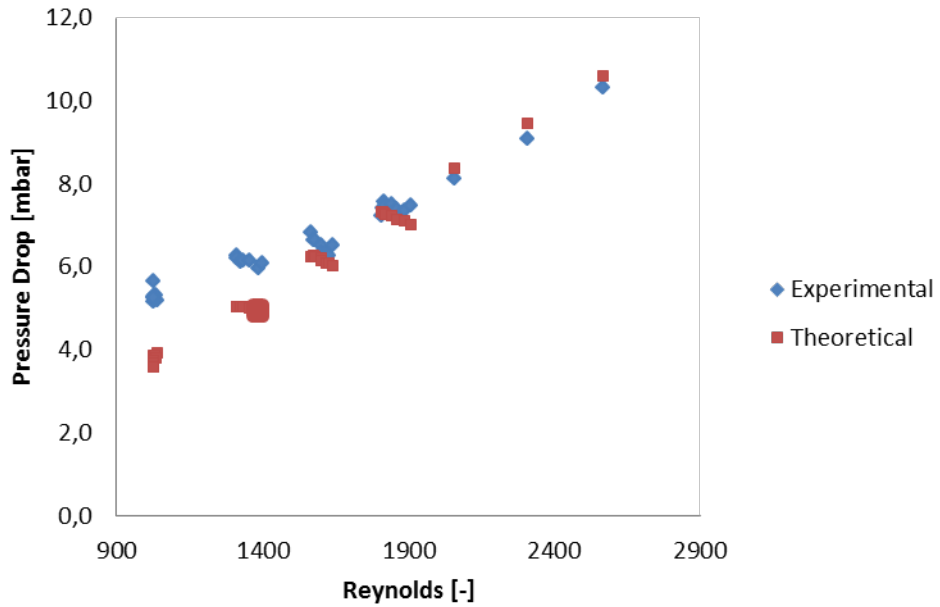


Fig.8. Experimental and theoretical pressure drops versus Reynolds dimensionless number

As expected, the experimental data is in reasonably good agreement with the classical macroscale theory for almost all Reynolds number. One point worth noting is that for very low Reynolds numbers (< 1300) this agreement seems to disappear, with the experimental pressure drop higher than the expected values. Another point is that both trends seem to keep a linear slope, even if theoretical points exhibit a higher direction coefficient than experimental ones.

Overall heat balance

The energy balance of the system has been performed, taking into account all the sections of the whole refrigerant loop. For each component or pipe section, the heat transfer exchange has been evaluated as

$$Q = \dot{m} \cdot c_p \cdot (T_{\text{section,out}} - T_{\text{section,in}})$$

where $T_{\text{section,out}}$ and $T_{\text{section,in}}$ are measured by the several thermocouples positioned around the R134a loop.

Table 3 shows the balances results. All the heat power measurement units are expressed in mW. It may be seen that, for all the tests performed, the sum of the heat power exchanges into the test rig is equal or very close to 0. This leads to the fair assumption that the system is correctly balanced.

Balance										
	Test	heat/ev	evap.	ev/cond	Conden.	cond/pump	pump	pump/heat	heat.	BALANCE
q	1	191,1	1496,5	3148,9	-19805,3	152,4	10492,3	3197,4	1126,8	2,27374E-12
	2	182,3	1917,3	2796,6	-19925,4	97,2	10650,6	3166,3	1115,0	1,81899E-12
	3	178,9	3313,5	2236,4	-20577,7	130,6	10511,8	3078,3	1128,1	0
	4	194,5	4778,1	1877,6	-21504,6	100,1	10213,1	3190,3	1150,9	0
	5	171,5	6737,4	1283,2	-23413,1	127,7	10921,1	3023,0	1149,3	0
	6	160,7	9960,0	-41,0	-25755,3	100,7	11275,6	3169,5	1130,0	0
	7	151,7	12067,6	-684,6	-27363,1	88,3	11341,7	3261,9	1136,5	0
	8	400,3	1519,3	2396,5	-18110,6	228,5	9144,9	3612,1	809,0	2,6148E-12
	9	441,8	2023,0	2283,5	-18270,4	167,6	8947,4	3626,2	780,8	3,29692E-12
	10	412,9	2786,2	1807,5	-18541,4	279,5	9101,6	3364,6	789,1	-2,72848E-12
	11	387,0	3870,0	1330,3	-19020,2	210,9	9316,9	3121,4	783,6	-1,13687E-12
	12	423,2	5107,9	809,3	-19441,1	28,0	9069,6	3243,9	759,2	-1,7053E-12
	13	420,6	6806,1	40,5	-20144,1	58,5	8813,6	3256,3	748,5	9,09495E-13
	14	407,5	8540,5	-762,7	-20980,1	129,6	8571,1	3376,9	717,2	3,06954E-12
	15	83,5	1978,1	4846,2	-25695,0	-58,5	12679,9	4477,3	1688,4	0
	16	95,0	2544,1	4653,1	-26028,5	-47,9	12727,8	4361,0	1695,5	-3,41061E-12
	17	85,1	3743,1	4328,8	-26972,6	7,4	13265,1	3832,9	1710,2	-1,81899E-12
	18	90,6	5785,4	3648,3	-28913,9	-5,0	13564,2	4127,3	1703,0	0
	19	121,2	7436,4	2990,6	-29413,3	45,5	12743,8	4397,2	1678,6	-2,50111E-12
	20	117,7	9965,7	2144,2	-31266,4	-106,7	12790,6	4599,4	1755,5	0
	21	100,8	12364,6	1231,7	-32304,1	-138,5	12442,6	4583,3	1719,5	0
	22	58,6	14796,6	253,0	-34185,5	14,3	12929,1	4450,2	1683,8	-2,04636E-12
	23	-78,2	1891,8	5261,4	-28125,1	-102,8	15045,3	4257,5	1850,1	-4,54747E-12
	24	-63,8	2652,9	5446,1	-29400,2	-193,0	15107,4	4514,5	1936,0	4,3201E-12
	25	-92,4	3704,7	5218,7	-30181,1	-183,6	15032,8	4552,7	1948,1	0
	26	-62,6	5123,7	4467,7	-30611,1	-266,8	14964,0	4468,7	1916,3	0
	27	-70,5	7512,2	3691,8	-32228,0	-309,4	15061,0	4427,7	1915,1	2,04636E-12
	28	-96,3	11102,0	2518,5	-34752,3	-219,4	15197,2	4375,7	1874,5	-3,86535E-12
	29	-131,9	13942,0	1572,5	-36685,5	-252,6	15306,7	4372,9	1875,9	-4,3201E-12
	30	-111,1	18176,3	8,4	-39473,8	-291,4	15368,9	4455,4	1867,4	2,50111E-12
	31	-54,4	2045,4	6155,6	-31131,1	-205,4	16732,1	4456,8	2001,1	0
	32	254,5	2317,8	7376,6	-35162,4	-326,7	18844,4	4794,4	1901,3	0
	33	484,1	2346,9	8210,3	-38317,5	-459,2	21006,2	4940,2	1789,0	-1,81899E-12

Table 3. Energy balance for the entire loop

5.2 Two-phase tests and results

Flow boiling (vertical upward flow) experiments have been performed for the rectangular channel of the dimensions 700x5000µm (hydraulic diameter of $D_h=1253\ \mu m$) of the heated length of 190 mm and R134a as a working fluid. The operating conditions are presented in the table 4.

Experiments were conducted for either fixed mass flux while changing heat flux in small steps or fixed heat flux and changing mass flux. All other parameters for a given set of experiments were fixed. The results of the experiments are presented in the figures below. Influence of heat flux on the heat transfer coefficient was studied for four working pressures and at least three mass flux settings for each set of data.

Parameter	Operational data range
P_{in} [bar]	5.9/6.5/7/7.5
T_{sat} [$^{\circ}$ C]	20/23/25/28
G [kg/m ² s]	190 - 350
q'' [kW/m ²]	2 - 100
$\Delta T_{subc,in}$ [$^{\circ}$ C]	4
x [-]	-0.1 – 0.9

Table 4. Operating conditions for the saturated flow boiling experiments

Local heat transfer coefficients as a function of heat flux and vapor quality for one specific set of data ($G=288$ kg/m²s $P_{sat}=6,5$ bar) are presented in Fig.9. It can be observed that apart from the data representing the inlet of the test section (negative and lowest x values, where heat transfer coefficient still increases with the heat added, indicating subcooled conditions), there is an obvious increase in the heat transfer coefficient with the heat flux and no or slight influence of the vapor quality. It has been also observed that for lower heat fluxes and just above the point where the ONB occurs, the values of heat transfer coefficient are higher than the values downstream. This can be explained by the increased heat transfer rate which occurs due to the onset of nucleate boiling.

The effect of mass flux on the average heat transfer values for one working pressure ($P_{sat}=7,5$ bar) and different heat and mass fluxes are presented in Fig.10. It is quite clear that heat transfer coefficient is independent of the mass flux and proves again that it is a function of heat flux.

In Fig.11 average heat transfer coefficient is plotted as a function of heat flux for four tested working pressures and one mass flux ($G=287$ [kg/m²s]). Here the strong dependence of the heat transfer coefficient on the heat flux is also proven and can also be seen that it increases on a smaller extent with the system pressure as well.

Boiling curves for selected data sets are plotted in Fig.12. Three trends can be distinguished from the graph: first, a convective heat transfer to the liquid followed by the convective boiling is observed for superheats of up to 3-5 degrees. When the boiling is established, wall temperature differences do not variate with more than one degree until the appearance of dryout, when the superheat starts increasing again, as in the case of the curve for $P=7$ [bar]& $G=240$ [kg/m²s], for example.

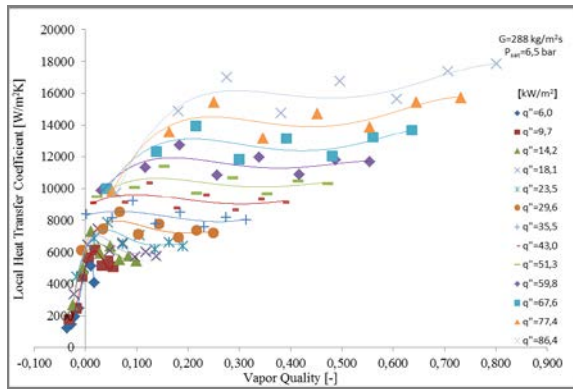


Fig.9. Local heat transfer coefficient as a function of vapor quality for different heat fluxes at $T_{sat} = 23 [{}^{\circ}\text{C}]$ and $G = 288 [\text{kg}/\text{m}^2\text{s}]$

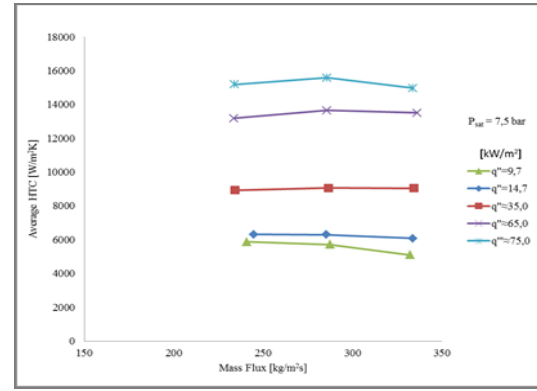


Fig.10. Average heat transfer coefficients as a function of mass flux for different heat fluxes at $T_{sat} = 28 [{}^{\circ}\text{C}]$

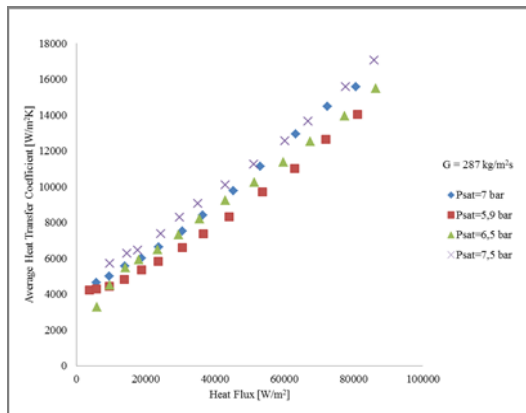


Fig.11. Average heat transfer coefficient as a function of heat flux at $G = 287 [\text{kg}/\text{m}^2\text{s}]$ for different pressures

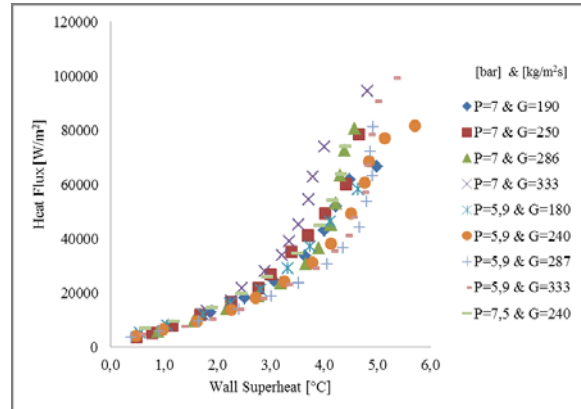


Fig.12. Boiling curve: heat flux plotted against wall superheat for three different pressures

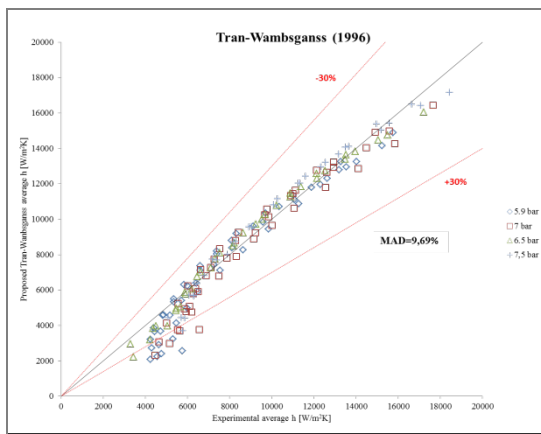


Fig.13. Comparison of the experimental heat transfer data against data predicted by Tran-Wambganss 1996 correlation

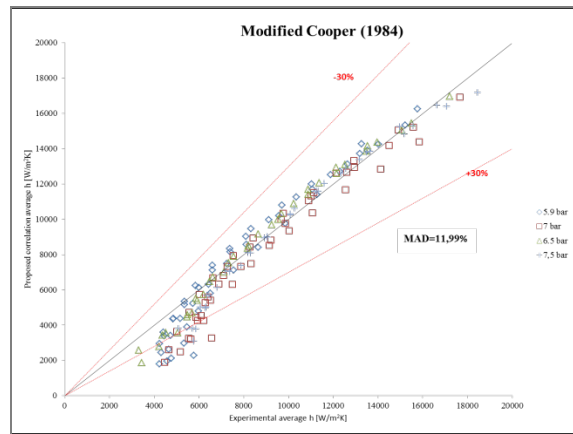


Fig.14. Comparison of the experimental heat transfer data against data predicted by Cooper 1984 modified correlation (with best fit $C_1 = 84,3$)

Experimental heat transfer coefficients were compared against 16 different correlations proposed in the literature for conventional and small channels. Best agreements were reached with Owhaib (2007) ($MAD=18,05\%$), Gungor-Wintherton (1986) ($MAD=17,71\%$) and Sun-Mishima (Modified Lazarek-Black) (2009) ($MAD=15,3\%$) correlations. However, the use of correlations of Cooper (1989) and Tran-Wambsganss (1996), modified to our data, have shown mean deviations of 11,99 and 9,69 % respectively. The coefficient C_1 in the Cooper (1989) correlation after data fit became 84,3 instead of 35, and in Tran-Wambsganss' (1996) correlation $C=1.4431\times 10^6$ instead of original 8.4×10^5 .

Two-phase pressure drop

The measured pressure drop that occurs in the test section has been compared to the predicted values from homogeneous model (in which the two-phase viscosity is taken from Cicchitti (1960) equation) and to the Müller-Steinhagen and Heck (1986) separated flow model. Results are shown in Fig.15 and Fig.16.

Both homogeneous and separated models tend to underestimate the measured pressure drop. Homogeneous model with Cicchitti's two-phase viscosity shows a MAD of 23%. Odd points mostly relapse in 5,9 bar experiments, whereas slightly better agreements are shown for higher system pressures.

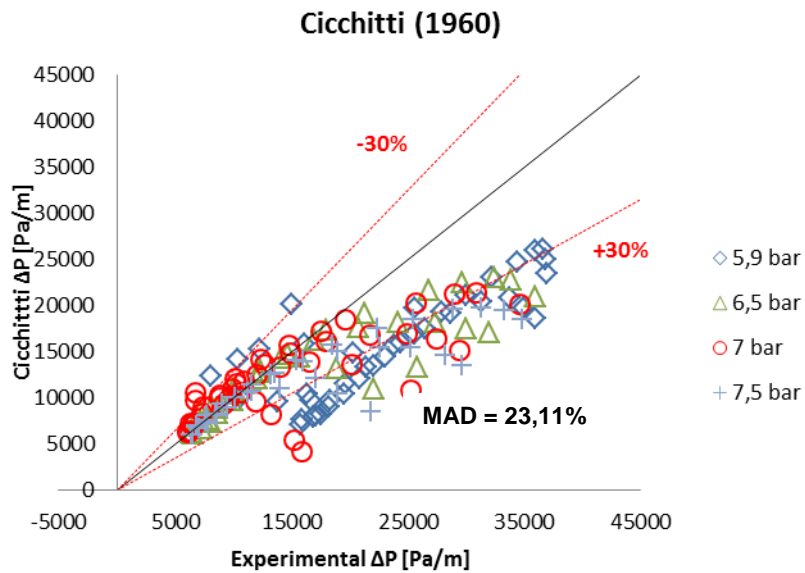


Fig.15 Comparison of the experimental pressure drop with homogeneous flow model

Müller-Steinhagen and Heck (1986)

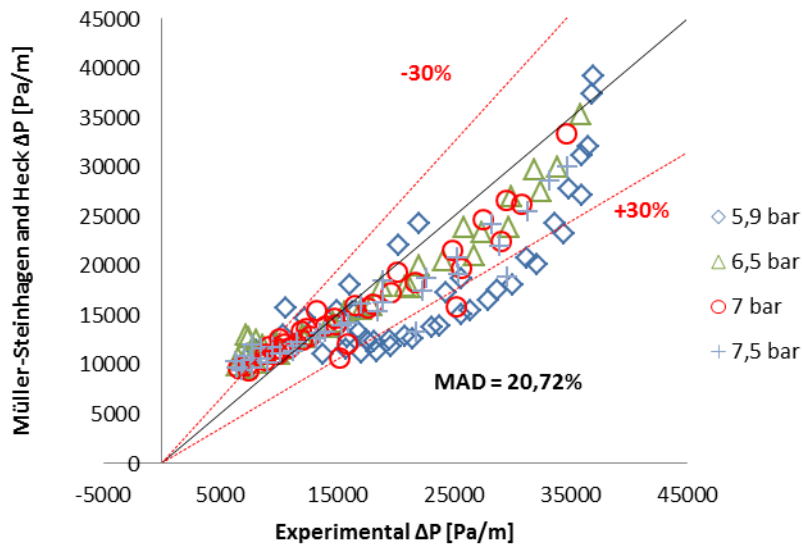


Fig.16 Comparison of the experimental pressure drop with separated flow model

This model is working properly for low heat fluxes and mass fluxes, thus for low values of the pressure drop, while great deviations appear for higher pressure gradients. Certainly, the assumption in the homogeneous model that the liquid and the vapor move with the same velocity is not valid, especially for high values of mass flux and heat flux, and thus for high pressure drops. The separated flow model shows a MAD of 21% circa. Better agreements are highlighted for great pressure drops, even if the model largely underestimates the experimental points, especially for tests performed at 5,9 bar. For low heat and mass fluxes, instead, the mean deviations are around 25% and the model overpredicts the measured values.

It is thus fair to say that these two models, even if developed for conventional pipes and characterized by their extreme simplicity, agree surprisingly well with experimental data.

6. Conclusions

Although the importance of micro-technology is growing bigger nowadays and the research on mini and micro-channels is booming, flow boiling data of any kind of refrigerant in narrow tubes are scarce as it can be seen from the literature survey. Therefore flow boiling of R134a in a vertical rectangular channel of small hydraulic diameter (1,253 mm) has been investigated in this thesis for a better understanding of the boiling phenomena in such types of geometry. In addition to literature reviews about the boiling process in micro-channels, an overall description of the test rig has been given. Then some tests in liquid single-phase flow have been performed in order to validate the experimental equipment: the results have shown that the test section is well insulated and there is a good equivalence between the heat power injected and the one absorbed by the working fluid. The most important results in terms of heat transfer coefficients and pressure drops, together with their comparisons with well-known correlations in literature are summarized below. In the end, some recommendations for future works are given.

33 tests in single-phase liquid refrigerant flow have been conducted. In agreement with classical theory for macro-scale, the heat transfer coefficient has been increasing with increasing Reynolds number and then mass flux, due to a major convective contribution, whereas the influence of heat flux is almost negligible. Shah-London (1978) correlation is quite in good agreement with the experimental heat transfer coefficients, though it underestimates real values for high Reynolds numbers. As regard the pressure drop, it has been seen to increase with Reynolds number and conventional macro-scale theory is in excellent agreement with the experimental data, especially for tests performed at high mass fluxes.

More than 160 flow boiling tests have been performed using several values for mass flux and system pressure in two-phase flow. For each of them, the heat flux has been increased from the lowest value able to make the fluid boil up to the extreme voltage of the main heater. Occasionally, dryout occurred.

It might be observed that at a fixed mass flux and system pressure, the heat transfer coefficient is highly dependent on the heat flux; in particular it increases with increasing heat flux and its influence is almost linear for all the saturated flow boiling experiments. On the contrary, mass velocity has no particular influence on the heat transfer coefficient, whereas vapour quality has only a weak effect: at low heat fluxes the heat transfer coefficients seem to decrease with increasing vapour quality, whereas it is quite stable for average heat fluxes. Sporadically, for $x > 0,55$, a slight increase of the local heat transfer coefficient is observed, probably due to the convective contribution which becomes more important with the boiling flow and the increasing velocity of the two phases. Sometimes, for very high heat fluxes and

vapour qualities, a partial dryout occurs and the heat transfer coefficient drops, due to intermittent gas layer on the inside walls of the channel. Tests performed with several system pressures show that this parameter has only a weak (though not negligible) effect on the heat transfer coefficient: it is increasing with increasing saturation pressure. The main reason should be investigated in the increasing number of nucleation sites, but additional factors may also be the effect of pressure on the latent heat of vaporization and liquid density.

The results obtained are in agreement with most of the experiments performed in micro-channels and reported in the literature review: the strong influence of the heat flux and the effect of saturation pressure, together with negligible consequences when varying vapor quality and mass flux, lead to the conclusion that the boiling process is mainly controlled by the nucleate boiling mechanism.

A comparison of experimental results with existing correlations has also been performed: mainly pool boiling equations and flow boiling formula based on nucleate boiling dominating effects have been used for this analysis. Best agreements are found for Gungor and Winterton (1985) and Sun-Mishima (2009) correlations, even if the first one was developed for conventional channels. The calculated MADs for these equations are 18% and 15%, respectively, while all other chosen correlations show deviations around 20-25%, quite surprising if considering that in micro-channels a 30% deviation still remains a good prediction. However, none of the correlations is able to predict exactly the experimental data and most of them are overestimating the real values; this is probably due to the fact that well-known correlations are not able to take into account parameters such as thermophysical properties of the fluid or the inside roughness of the channel. Cooper (1984) and Tran-Wambsganss (1996) equations have been optimized for the present data by changing the initial constant with a best-fit regression. New calculated MADs are 12% and 10%, respectively.

As regard the diabatic two-phase pressure drop, experimental values have been compared with the homogeneous flow model using Cicchitti (1960) two-phase viscosity and with the separated flow model developed by Müller-Steinhagen and Heck (1986). Both correlations work reasonably well: homogeneous flow model gives a MAD of 23% and separated flow model leads to a MAD of 21%, quite unexpected since they have been developed for conventional tubes. However, some other models especially created for micro-channels would need to be studied as well.

Future work

Although in this project several correlations have been proven to predict reasonably well the heat transfer coefficient values, further research is still needed before flow boiling heat transfer processes in narrow tubes are fully understood.

First of all, the influence of the channel hydraulic diameter or at least its aspect ratio is not investigated in this work, as well as the influence of the working fluid, since

R134a is the only refrigerant utilized for all the tests, in single-phase and boiling flows. It might be interesting to observe how these two parameters can modify the heat transfer coefficient.

Secondly, more experiments should be done to further validate the proposed correlations developed in this thesis for the present experimental facility.

Thirdly, it might be useful to change the heated length of the channel and to investigate about dryout incipience and critical heat flux values.

Finally, more heat transfer studies together with flow visualization are strongly recommended, in order to develop new models based on the physics of the boiling process combined with a flow pattern regimes analysis. This might be the right way to fully understand the boiling phenomena in compact heat exchangers.

Referenses

- Bao Z.Y., Fletcher D.F., Haynes B.S., (2000). *Flow boiling heat transfer of freon R11 and HFCFC123 in narrow passages*. Int. J. Heat Mass Transfer 43, 3347–3358.
- Brauner N., Maron D.M., (1992). *Identification of the Range of 'Small Diameters' Conduits, Regarding Two-Phase Flow Pattern Transitions*. International Communications in Heat and Mass Transfer 19(1): 29-39.
- Bui T.D., Dhir V.K., (1985). *Transition boiling heat transfer on a vertical surface*. J. Heat Transfer, 107, 756–763.
- Callizo M.C., Palm B., Owhaib W., Ali R., (2010). *Flow Boiling Visualization of R-134a in a Vertical Channel of Small Diameter*. Journal of Heat Transfer 132(3): 031503-8.
- Cataldo F., (2012). *Boiling flow pattern characterization in a vertical single microchannel*. Department of Energy technology, Stockholm, Sweden, Royal Institute of Technology, KTH. Master thesis.
- Chen J.C., (1966). *Correlation for boiling heat transfer to saturated fluids in convective flow*. AIChE Proc. Des. Dev. 5(3), 322-329.
- Cicchitti A., Lombardi C., Silvestri M., Soldaini G., Zavalluilli R., (1960). *Two-phase cooling experiments pressure drop, heat transfer and burnout measurements*. Energia Nucleare, Vol. 7, 407-425.
- Collier J.G., Thome J.R., (1994). *Convective boiling and condensation, 3rd Edition*. Oxford Science Publications, 1-33, 131-182, 183-213, 325-374.
- Cooper M.G., (1984). *Saturation nucleate pool boiling – a simple correlation*. 1st UK National Heat Transfer Conference (I. Chem. E. Symp. Series No. 86) 2, 785-93.
- Cooper M.G., (1989). *Flow boiling –the “apparently nucleate” regime*. Int. J. Heat Mass Transfer 32, 459-464.
- Dukler A.E., Wicks M.III, Cleveland R.G., (1964). *Frictional pressure drop in two-phase flow: (a) A comparison of existing correlation for pressure loss and holdup, (b) An approach through similarity analysis*. AIChE J., Vol. 10, 38-51.
- Feng Z., Serizawa A., (2000). *Two-phase flow patterns in ultra-smallchannels*. In: Second Japanese–European Two-Phase Flow Group Meeting, Tsukuba, Japan.

Gnielinski V., (1995). *Ein neues Berechnungsverfahren für die Wärmeübertragung im Übergangsbereich zwischen laminarer und turbulenter Rohrströmung*. Forschung im Ingenieurwesen-Engineering Research, Vol 61.

Gungor K.E., R. Winterton H.S., (1986). *A general correlation for flow boiling in tubes and annuli*. Int. J. of Heat and Mass transfer, Vol. 29, No. 3, 351-358.

Harirchian T., Garimella S.V., (2010). *A Comprehensive Flow Regime Map for Microchannel Flow Boiling with Quantitative Transition Criteria*. International Journal of Heat and Mass Transfer 53(13-14), 2694-2702.

Hsu Y.Y., Graham R.W., (1963). *A visual study of two-phase flow in a vertical tube with heat addition*. NASA Technical Note D-1564.

Jacobi A.M., Thome J.R., (2002). *Heat transfer model for evaporation of elongated bubble flows in microchannels*. J. Heat Transfer 124, 1131–1136.

Jung D.S., McLinden M., Radermacher R., Didion D., (1989). *A study of flow boiling heat transfer with refrigerant mixtures*. Int. J. Heat Mass Transfer 32, 1751-1764.

Kandlikar S.G., (1990). *A general correlation for saturated flow boiling in horizontal and vertical tubes*. Trans. ASME 112, 219–228.

Kandlikar S.G., Grande W.J., (2003). *Evolution of Microchannel Flow Passages-Thermohydraulic Performance and Fabrication Technology*. Heat Transfer Engineering 24(1), 3 – 17.

Kandlikar S.G., Chung J.N., (2006). *Multiphase Flow Handbook*. CRC Press, Taylor and Francis Group Boiling and Condensation –Chapter 3.

Kew P.A., Cornwell K. (1997). *Correlations for the Prediction of Boiling Heat Transfer in Small-Diameter Channels*. Applied Thermal Engineering 17(8-10), 705-715.

Kuwahara K., Koyama S., Yu J., Watanabe C., Osa N., (2000). *Flow pattern of pure refrigerant HFC134a evaporating in a horizontal capillary tube*. In: Proceedings of Symposium on Energy Engineering in the 21st Century, Hong Kong, vol. 2, 445–450.

Lazarek G.M., Black S.H., (1982). *Evaporative heat transfer, pressure drop and critical heat flux in a small vertical tube with R-113*. Int. J. Heat Mass Transfer 25, 945–959.

Li W., Wu Z., (2010). *A general correlation for evaporative heat transfer in micro/minichannels*. Int. J. of Heat and Mass Transfer 53, 1778-1787.

Liu Z., Winterton R.H.S., (1991). *A general correlation for saturated and subcooled flow boiling in tubes and annuli, based on a nucleate pool boiling equation*. Int. J. of Heat and Mass Transfer, Vol. 34 (11), 2759-2766.

Maqbool M.H., Palm B., Khodabandeh R., (2013). *Investigation of two phase heat transfer and pressure drop of propane in a vertical circular minichannel*. Experimental Thermal and fluid Science 46, 120-130.

McAdams W.H., Woods W.K., Heroman L.C., (1942). *Vaporization inside horizontal tubes- Benzene-oil mixture*., ASME Transaction, Vol. 64, 193-200.

Mehendale S.S., Jacobi A.M., Shah R.K., (2000). *Fluid Flow and Heat Transfer at Micro- and Meso-Scales with Application to Heat Exchanger Design*. Applied Mechanics Reviews 53(7), 175-193.

Müller-Steinhagen H., Heck K., (1986). *A simple friction pressure drop correlation for two-phase flow in pipes*. Chem. Eng. Process, Vol. 20, 297-308.

Nukiyama S., (1934). *The maximum and minimum values of heat Q transmitted from metal to boiling water under atmospheric pressure*. J. Jpn. Soc. Mech. Eng., 37, 367–374.

Owhaib W. (2007). *Experimental heat transfer, Pressure Drop and flow visualization of R134a in vertical mini/micro tubes*. Department of Energy Technology. Stockholm, Sweden, Royal Institute of Technology, KTH. Doctoral thesis.

Palm B., (1991). *Enhancement of boiling heat transfer by aid of perforated metal foils*. Department of Energy Technology. Stockholm, Sweden, Royal Institute of Technology, KTH. Doctoral thesis.

Palm B., (2002). *Heat transfer in heat exchangers designed for minimum charge*. Zero Leakage – Minimum charge, IIR/IIF, Royal Institute of Technology, Department of Energy Technology, Stockholm, Sweden.

Rohsenow W.M., (1952). *A method of correlating heat transfer data for surface boiling of liquids*. Trans. ASME, 74, 969.

Rouhani S.Z., Axelsson E., (1970). *Calculation of void volume fraction in subcooled and quality boiling regions*. Int. J. Heat Mass Transfer 18, 381-393.

Shah R.K., (1986). *Classification of heat exchangers*. In heat exchangers: Thermal-Hydraulic Fundamentals and Design (Edited by S. Kakac, A. E. Bergles & F. Mayinger), Hemisphere Publishing Corp., Washington, DC, 9-46.

Shah R.K., London A.L., (1978). *Laminar Flow Forced convection in Ducts*. Academic Press.

Shah R.K., Sekulic D.P., (2003). *Fundamentals of heat exchanger Design*. John Wiley & Sons, 475-481.

Stephan K., Abdelsalam M., (1980). *Heat transfer correlations for natural convection boiling*. Int. J. Heat mass transfer, 23, 73-87.

Stephan P., Hammer J., (1994). *A new model for nucleate boiling heat transfer*. Int. J. Heat Mass Transfer 30, 119-125.

Sun L., Mishima K., (2009). *An evaluation of prediction methods for saturated flow boiling heat transfer in mini-channels*. Int. J. Heat Mass Transfer 52. 5323–5329.

Thome J.R., (2004-2010 a). *Engineering Data Book III*, Chap. 4, Wolverine Tube, 27p.

Thome J.R., (2004-2010 b), *Engineering Data Book III*, Chap. 13, Wolverine Tube, 34p.

Thome J.R., Dupont V., Jacobi A.M., (2004). *Heat Transfer Model for Evaporation in Microchannels. Part I: Presentation of the Model*. International Journal of Heat and Mass Transfer 47(14-16), 3375-3385.

Tran T.N., Wambsganss M.W., France D.M., (1996). *Small circular and rectangular channel boiling with two refrigerants*. Int. J. Multiph. Flow 22. 485–498.

Warrier G.R., Dhir V.K., Momoda L.A., (2002). *Heat transfer and pressure drop in narrow rectangular channels*, Exp. Thermal Fluid Sci. 26, 53–64.

Webb R.L., Gupte N.S., (1992). *A critical review of correlations for convective vaporization in tubes and tube banks*. Heat Transfer Eng. 13, 58-81.

Yu W., France D.M., Wambsganss M.W., Hull J.R., (2002). *Two-phase pressure drop, boiling heat transfer, and critical heat flux to water in a small-diameter horizontal tube*. Int. J. Multiphase Flow 28, 927–941.

Projektets vetenskapliga publikationer

Cataldo, F., (2012), *Study on visualization of flow patterns during boiling of R134a in a high aspect ratio rectangular single channel*, MSc thesis, electronic copy, Supervisor: Samoteeva, O.

Landron, B, (2013), *Heat transfer in boiling in microchannels*, Msc thesis, electronic copy. Supervisor: Samoteeva, O.

Samoteeva, O., Palm, B. (2014), *Heat transfer during refrigerant boiling in single mini channels of a rectangular shape*, Proceedings of the 5th International Conference on HEAT TRANSFER and FLUID FLOW in MICROSCEALE, Marseille, France, Apr. 22-25, 2014, poster presentation

Samoteeva, O., Palm, B. (2014), *Heat transfer and pressure drop during refrigerant boiling in single mini channels of a rectangular shape*, to be submitted to The Journal of Experimental Thermal and Fluid Science, August 2014

Viscito, L, (2014), *Experimental study on heat transfer during flow boiling of refrigerant R134a in a small rectangular channel*, MSc thesis, electronic version, Supervisor O.Samoteeva

Projektets populärvetenskapliga publikationer och presentationer

Samoteeva, O., Palm. B., (2012) *Study on heat transfer, pressure drop and flow behavior visualization during evaporation in small channels of a rectangular shape*, Poster presentation, "Svenska Kyl- och Värmepumpdagen 2012", October 19 2012, Göteborg.

Samoteeva, O. (2013) *Latest results on heat transfer and pressure drop during boiling in rectangular micro channels*, Presentation at the Huawei Global Electronic Cooling Technology Workshop, September 2013

Samoteeva, O., Palm, B., (2013) *Study on heat transfer, pressure drop and flow behavior visualization during flow boiling in small rectangular channels*, Poster presentation, October, 18, 2013, EFFSYS+ dagen, Göteborg

Samoteeva, O., (2013) *Why bubbles are important to our comfort*, Poster presentation, November, 7, 2013, Energy Dialogue, KTH, Stockholm

Samoteeva, O., (2013) *Why bubbles are important to our comfort*, Pitch presentation, November, 7, 2013, Energy Dialogue, KTH, Stockholm

Samoteeva, O., (2013) *Boiling in Microchannels: Now and in the Future*, Our research made comprehensible: Texts from the course "Communication Skills for Energy", USAB, Stockholm 2013

APPENDIX 1

Nomenclature

Roman

A	Cross-sectional area [m^2]
a_r	Aspect ratio [-]
CHF	Critical heat flux [W/m^2]
c_p	Heat capacity [$\text{J}/(\text{kgK})$]
D_h	Channel hydraulic diameter [m]
d_0	Bubble departure diameter [m]
E	Enhancement factor [-]
f	Friction factor [-]
F	Enhancement factor [-]
F_{fl}	Fluid-surface parameter [-]
g	Gravitational acceleration [m/s^2]
\dot{G}	Mass flux [$\text{kg}/(\text{m}^2\text{s})$]
h	Heat transfer coefficient [$\text{W}/(\text{m}^2\text{K})$]
I	Current [A]
L	Test section length [m]
M	Molecular weight [kg/kmol]
\dot{m}	Mass flow rate [kg/s]
P	Pressure [bar]
P_r	Reduced pressure, P/P_{cr} [-]
Q	Heat power [W]
q''	Heat flux [W/m^2]
Ro	Surface roughness [μm]
s	Standard deviation
S	Suppression factor [-]
T	Temperature [$^\circ\text{C}$]
u	Uncertainty

V	Voltage [V]
w	Systematic uncertainty
x	Vapor quality [-]
z	Axial position [m]
z_0	Position where boiling starts [m]

Greek

Δh_{VL}	Latent heat of vaporization [J/kg]
ΔP	Pressure drop [mbar]
ΔT	Temperature difference [$^{\circ}\text{C}$]
ΔT_{sat}	Wall superheat, $T_{\text{wall}} - T_{\text{sat}}$ [$^{\circ}\text{C}$]
Δx	Vapor quality difference [-]
ε	Void fraction [-]
λ	Thermal conductivity [W/(mK)]
μ	Dynamic viscosity [Pa s]
ρ	Density [kg/m ³]
σ	Surface tension [N/m]
Ψ	Cross sectional perimeter [m]

Subscripts

acc	Acceleration
$ave/mean$	Average
cb	Convective boiling
cr	Critical
$fluid$	Bulk fluid
fr	Friction
G	Gas phase
in	Inlet section
$inwall$	Internal wall
L	Liquid phase
nb	Nucleate boiling

<i>out/ex</i>	Outlet section
<i>outwall</i>	External wall
<i>pool</i>	Pool boiling
<i>preh</i>	Pre-heater section
<i>sat</i>	Saturated conditions
<i>sp</i>	Single-phase
<i>st</i>	Static
<i>tot</i>	Total
<i>tp</i>	Two-phase
<i>wall</i>	Wall

Dimensionless parameters and definitions

<i>Bo</i>	Boiling number $\frac{q''}{g \cdot \Delta h_{VL}}$
<i>BO</i>	Bond number $\frac{D_h^2 \cdot g \cdot (\rho_L - \rho_G)}{\sigma}$
<i>Co</i>	Confinement number $\sqrt{\frac{\sigma}{g \cdot (\rho_L - \rho_G)}} \cdot \frac{1}{D_h}$
<i>MAD</i>	Mean Absolute Deviation $\frac{1}{n} \cdot \sum_{i=1}^n \frac{ h_{predicted} - h_{experimental} }{h_{experimental}}$.
100	
<i>Nu</i>	Nusselt number $\frac{h \cdot D_h}{\lambda}$
<i>Po</i>	Poiseuille number $f \cdot Re$
<i>Pr</i>	Prandtl number $\frac{\mu \cdot c_p}{\lambda}$
<i>Re</i>	Reynolds number $\frac{\dot{G} \cdot D_h}{\mu}$
<i>We</i>	Weber number $\frac{\dot{G}^2 \cdot D_h}{\rho_L \cdot \sigma}$
<i>X_{tt}</i>	Martineli parameter $\frac{\left(\frac{dP}{dz}\right)_L}{\left(\frac{dP}{dz}\right)_G}$